Applied Thermal Engineering 216 (2022) 119128

Contents lists available at ScienceDirect

Applied Thermal Engineering

journal homepage: www.elsevier.com/locate/apthermeng

Research Paper

Experimental investigation on the start-up performance of a loop heat pipe with three flat disk evaporators combined

Tong Wu, Tingting Wang, Zhengyuan Ma, Zikang Zhang, Wei Liu, Zhichun Liu *

School of Energy and Power Engineering, Huazhong University of Science and Technology, Wuhan 430074, China

ARTICLE INFO

Keywords:
Multiple-evaporator loop heat pipe
Multiple heat sources
Electronics cooling

ABSTRACT

To promote the heat transport applicability of the loop heat pipe(LHP) for high power and multi-heat sources, a multi-evaporator loop heat pipe(ME-LHP) system with three flat disk evaporators equipped with separate vapor lines was proposed and experimentally studied for the first time. The effects of the interaction between evaporators, the heat load distribution, and the gravity-assisted angle on the startup behavior of ME-LHP were investigated respectively. The results show that with the separated-vaporline structure, the adverse impact between evaporators was greatly reduced. The best performance appeared when all three evaporators were involved. At unequal heat load working conditions, the ME-LHP obtained the optimal startup performance when high heat load was applied on evaporators with a superior position in liquid separation. Besides, the outlet temperature of all evaporators tended to be consistent, even if multiple evaporators worked under unequal heat loads. The gravity-assisted angle affected the start-up process by changing the non-uniformity of liquid distribution. Compared with the gravity-assisted tilt $\theta = 10^{\circ}$, the highest performance was improved by 77 % for $\theta = 2^{\circ}$, and the peak load could reach 300 W. The present study may extend the application of the flat plane type of loop heat pipe for solving the multi-heat-sources dissipation problem.

1. Introduction

The development of high-power integration in electronic devices results in a severe growth in the generation of heat flux. Loop heat pipe (LHP), as a highly efficient two-phase heat transfer device without any movable components, has been widely applied to solve the high heat-flux problem[1–4].

The evaporator is usually divided into two types by its shape, flat and cylindrical[5]. Flat evaporators, without requiring any additional saddle for tight thermal contact with flat heat sources, can fully fit with the surface of electronic devices. Therefore, the structure of the system is greatly simplified and the thermal resistance is also reduced[6]. Due to the above benefits, the flat evaporator LHP has been continuously studied and investigated over the past few decades. Maydanik et al. [5] summarized the research status of flat evaporator LHP from the aspects of the material, working fluid, and also the wicks in evaporators. Two main types of flat evaporators were defined, one type was evaporators with opposite replenishment (EORs) and the other was evaporators with longitudinal replenishment (ELRs). And the best operation characteristics were found by the combination of steel-nickel-ammonia when the temperature was below 70 °C and copper–copper-water when the temperature was above 70 °C. Li et al. [7] designed a flat square evaporator and experimentally investigated the start-up process of the system when subjected to different heat loads. And the possible mechanism behind the different startup phenomena was proposed. He et al. [8] proposed a stainless steel LHP equipped with both primary wick and secondary wick, and ammonia was chosen as the working fluid. With the combination of them, the temperature oscillation was restrained and rapidly responded to the heat load changes. Odagiri et al. [9] designed a LHP with flat rectangular evaporator, and the system was tested under six different orientations. Results showed that when high heat flux was applied, the performance could be significantly affected by the orientation and liquid–vapor distribution. To meet the demands of long-distance heat transfer, Zhang et al. [10] proposed a LHP with flat disk evaporator, whose effective heat transfer distance could reach 1620 mm. The capillary force was provided by a bi-porous wick. During the tests, the loop operated stably from 2.5 W to 180 W. Zhao et al. [11] selected R1233zd(E) as the working fluid for an aluminum alloy flat evaporator LHP. The system still showed great performance even under relatively bad conditions (heat sink temperature was 30 °C).

Though loop heat pipe with one evaporator can meet the demand of

* Corresponding author.
E-mail address: zcliu@hust.edu.cn (Z. Liu).

https://doi.org/10.1016/j.applthermaleng.2022.119128
Received 1 March 2022; Received in revised form 1 August 2022; Accepted 4 August 2022
Available online 8 August 2022

Nomenclature

d	Pipe diameter (m)
d_w	Mesh diameter (m)
h	Heat transfer coefficient (W/ (m^2 • K))
K	Permeability (m^2)
N	Evaporator number
P	Pressure (Pa)
Q	Thermal power (W)
r	Capillary radius (m)
R	Thermal resistance (K/W)
Re	Reynolds number
u	Velocity (m/s)

Greek symbols

α	Void fraction of the compensation chamber
β	Liquid fraction of the compensation chamber
ε	Porosity
ρ	Density (kg/ m^3)
μ	Dynamic viscosity (Pa • s)
σ	Surface tension (N/ m)
θ	Contact angle (°)
φ	Welding coefficient

Subscripts

c	Cold case
cap	Capillary wick
cc	Compensation chamber
cl	Condenser line
cond	Condenser
evap	Evaporator
g	Gravity
gr	Vapor grove
h	Hot case
i	Number of evaporators
l,c	Densities of liquid in the worst cold case
l,h	Densities of liquid in the worst hot case
l	Liquid
ll	Liquid line
loop	Loop heat pipe
v	Vapor
v,c	Densities of vapor in the worst cold case
v,h	Densities of vapor in the worst hot case
vl	Vapor line
w	Wick

Abbreviations

C	Condenser
CC	Compensation Chamber
CPL	Capillary pumped loopy pumped loop
DC	Direct current
E1	Evaporator 1
E2	Evaporator 2
E3	Evaporator 3
LHP	Loop heat pipe
ME-LHP	Multi-evaporator Loop heat pipe
NCG	Non-condensable gas

high heat-flux requirements, there still remain some problems. When faced for multi-heat sources application scenarios such as future aircraft, large space stations and computing servers, where the high heat flux can even reach 150 W(6.35 W/cm^2) and the installation space is limited [1,12], the traditional loop heat pipe with single one evaporator is not suitable. Therefore, the multi-evaporator loop heat pipe was proposed to address such heat dissipation problems.

Currently, there are mainly-two types of LHP designed for multi-heat sources: Multi-stages LHP[13] and Multi-evaporator LHP[14], the main difference between them lies in weather evaporators are added. In multi-stage LHP without increasing the number of evaporators in the system, the additional heat exchangers can control the phase state of the working fluid, thus cooling several heat sources. Unlike the Multi-stage LHP, the Multi-evaporator LHP dissipates heat from multi-heat sources by increasing the number of evaporators, which has distinct advantages such as higher system flexibility, heat-load-sharing mode, and robust serviceability[15]. For the reasons mentioned above, ME-LHP becomes more suitable to high heat flux occasions such as spacecraft and high-power electronic applications.

Maydanik et al. [16] first proposed the ramified system which contained more than one evaporator in CPL and extended the design idea to LHP. Afterwards, the feasibility of the multi-evaporator loop heat pipe system was proven through theoretical studies and experimental validation[17]. And Bugby et al. [18,19] systematically summarized the distinctive and unique features of ME-LHP.

At present, most of the ME-LHP systems are derived and developed from conventional single-evaporator LHP, whose multiple evaporators are in parallel and were equipped with its own compensation chamber (CC), and the number of the condenser in system can be one or more. In pipe arrangement, multiple evaporators' outlets are usually connected with each other and share one vapor line, that means, the vapor will first converge and then enter the condenser. Liquid lines are usually equipped with branches for dividing working fluid.

Apparently, since ME-LHP systems have multiple branches, how to ensure good fluid supply to each branch is quite problematic. As the component directly supplies working fluid to evaporators, CC's volume size is crucial for achieving stable flow. Maydanik et al. [17] proposed that CC volume should be able to adapt the volume change of working fluid under the extreme hot and extreme cold case of system operation, so they considered the CC volume as a function of the components' volume and the density of the working fluid. The number of evaporators was added to the equation by Yun et al. [20] and they found by calculation that the number of evaporators had a great effect on the CC volume, which will increase sharply with the increase of the evaporators' number. According to the researchers, the relation between the CC volume and evaporators' number greatly limits the increase of the number of evaporators. Okutani et al. [21] took the two-phase state of the working fluid inside the system into consideration, and therefore two variables, the fractions of CC volume occupied by gas and liquid, were introduced into the equation which are proposed for LHP system with two evaporators. In 2015, a novel concept of ME-LHP which contained four evaporators was proposed by Hoang and Ku et al. [1] and by linking CCs together, the limitation of the number of evaporators because of the CCs volume sharply increase was broken. In addition, the required CC volume was greatly reduced compared with the conventional ME-LHP.

The start-up characteristics of an ME-LHP are quite important, especially when the system started at some unfavorable situation such as started at non-symmetric heat loads and unfavorable initial vapor–liquid distribution. Hence, a series of studies focused on the start-up characteristics of ME-LHP have been carried out. Qu et al.[22] experimentally analyzed the start-up characteristics of a DE-LHP, including four factors such as the interaction between evaporators, the heat load distribution and the wick seal. And Qu et al.[23] also investigated the start-up characteristics by proposing a steady-state model of a DE-LHP, which further explained the start-up characteristics of the ED-LHP. Hoang and

Ku et al. [1] studied the behavior of CCs in ME-LHP during the start-up period. The test results proved that there was always only one CC in control of the saturation temperature and at the same time the saturation control would switch among each CC. It was hard to predict which CC would control the saturation temperature because it could be affected by various factors, such as heat load distributions, the distance between the condenser and so on. Chang et al. [24] conducted a visualization test to confirm the effects of the phase state of working fluid in evaporators and CCs on the DE-LHP start-up characteristics. The results showed that there were two modes called gravity-driven mode and capillary-gravity-driven mode when the DE-LHP started, the distribution of vapor–liquid phase would greatly effect the start-up characteristics of the DE-LHP.

For research concerning the positioning of ME-LHP, tests at different orientations were carried out by Maydanik et al. [14], containing horizontal position, anti-gravity vertical position, and special horizontal position. The temperatures of the two CCs and two evaporators remained different even at the same heat load. Nguyen et al. [25] investigated a dual flat-evaporator loop heat pipe, and conducted tests in various orientations. Temperatures of the CCs were carefully investigated in detail, to confirm the vapor/liquid distribution in the CCs. The temperatures were not uniform at each evaporator causing by the two-phase state differences.

But the recent studies of multi-evaporator loop heat pipe were concerned mostly on cylindrical evaporators, the experiments on flat plane type multi-evaporator loop heat pipe are lacking. Besides, the arrangement of the pipe line used in cylindrical ME-LHP is not suitable anymore, and the vapor convergence way can cause high pressure loss in the system at the same time.

A multi-evaporator LHP with three flat plane type evaporators was investigated and tested for the first time to investigate the operating characteristics of flat plane type ME-LHP and extend the application of the flat plane type of LHP for solving the multi-heat-sources dissipation problem. In the experiment, the combination “stainless steel-nickel-ammonia” was chosen. The effects of the interaction between evaporators, the heat load distribution, and the gravity-assisted angle on the startup behavior of ME-LHP were investigated respectively. And some interesting phenomena were observed for the first time.

2. Experimental setup

2.1. ME-LHP system design

Involved from LHP, the ME-LHP system can be divided into two typical types, depending on whether the compensation chamber(CC) is used in common[14]. But in both two types, the vapor and liquid lines will always converge before meeting the junction. In this way, the mass and heat can fully exchange between branches. Therefore, the heat load sharing mode can be possible[24]. But at the same time, the complex interactions between each line could also cause the startup and operation processes become more complicated and unstable. Especially, the flat-shaped evaporators can be more sensitive disturbance due to the limitation of evaporator volumes.

As mentioned above a novel designed ME-LHP with three evaporators was proposed. As depicted in Fig. 1, the first distinguishing characteristic of the innovative ME-LHP system was that each evaporator was equipped with separate transport lines due to the greater flow resistance and higher pressure drop loss in vapor lines compared to liquid lines. Separated vapor lines can avoid excessive disturbance when vapor reaches the junction. In this manner, we can ensure that the system functions normally even if not all evaporators start simultaneously. In addition, convergence after the condenser can reduce the high-pressure drop caused by the high-speed flow of the working fluid, which guarantees the successful startup of the system. Secondly, the existence of a liquid separator can also be beneficial to the operation by buffering the working fluid and giving more freedom in fluid distribution. In order to realize mass and heat transfer between each line and evaporator to reach high heat transfer efficiency, a junction after the condenser has been adopted.

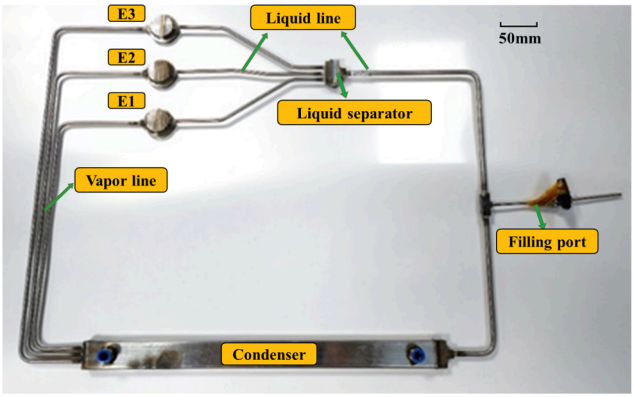

Fig. 1. System diagram of the flat disk ME-LHP.

2.2. ME-LHP sample

The three evaporators in the system were all disk-shaped(Fig. 2). Considering the compatibility with the ammonia working fluid, the material was SUS 316L. The evaporator and the CC were separated by the bi-porous wick. The rib on the evaporator heating surface cover plate was in close contact with the wick and was connected by welding.

The bi-porous wicks with two-size pore scales used in this experiment were comprised of nickel particles to provide capillary pump power, which was significantly more potent than the mono-porous capillary structure. The pore size distribution tested by mercury intrusion method, and the permeability was calculated according to Carman-Kozeny formula[26].

$$k = \frac{d^2\varepsilon^3}{180(1-\varepsilon)^2} \tag{1}$$

where k is the permeability of wicks, d is the mean pore diameter, and ε is the wick porosity. The detailed parameters for three wicks used in the experiment was provided in Table.1. Because of the existence of both large pores and small pores in the bi-porous wicks, the capillary pumping power was improved and the flow resistance was decreased [27].

All components in the system were made of SUS 316L. Ammonia was selected as the working fluid, considering the aim to control the heating surface at a lower temperature. The system diagram of the flat disk ME-LHP is shown in Fig. 3, and the main design parameters of the ME-LHP experiment are summarized in Table 2.

Charge ratio is a key design parameter for both LHP and ME-LHP systems. On the one hand, the charge ratio significantly affects the initial two-phase state in the loop, which can directly influence the start-up and operation characteristics of ME-LHP. On the other hand, the ME-LHP system has its own particularity. With the assumption of a two-phase state in only one CC and liquid-filled state in the other CCs, the fluid mass was calculated based on the worst cold case and worst hot case, given by [28]:

$$M_c = \rho_{l,c}\left(V_{loop} + (N-1)V_{cc}^i + \beta V_{cc}^i\right) + \rho_{v,c}(1-\beta)V_{cc}^i, \tag{2}$$

$$M_h = \rho_{l,c}\left(V_{ll} + \varepsilon V_w + (N-1)V_{cc}^i + (1-\alpha)V_{cc}^i\right) + \rho_{v,h}\left(\alpha V_{cc}^i + V_{gr} + V_{vl} + V_{cl}\right), \tag{3}$$

where V_{loop} is the loop total volume, excluding the CCs, V_{cc}^i is the volume of the CC^i, i is the number of evaporators, β is the liquid fraction of the

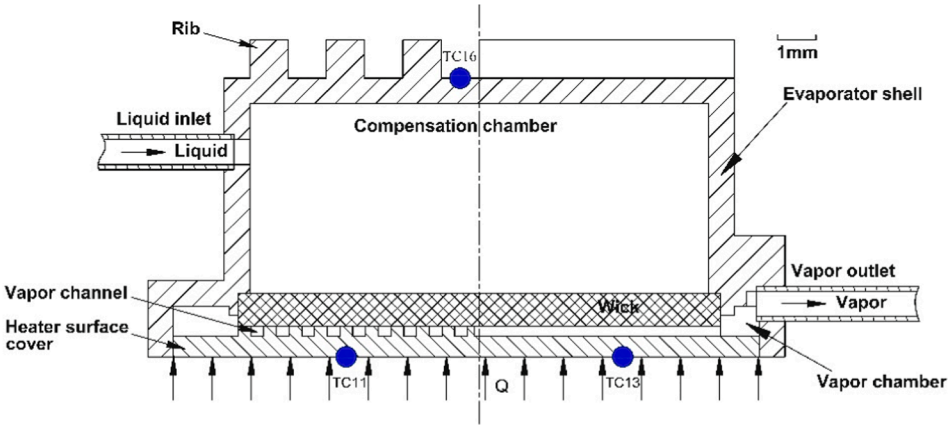

Fig. 2. The configuration of the evaporator.

Table 1
Pore radius and permeability of the wicks used in the experiment.

Wick	$D_{large\ pores}$/μm	$D_{small\ pores}$/μm	$D_{equivalent\ pore}$/μm	permeability /m^2	Thermal conductivity/ (W/m·K)	Thermal resistances/(m^2·K/W)
Wick 1	8.12	2.6	3.35	2.96×10^{-13}	2.64	6.29×10^{-4}
Wick 2	8.67	2.8	3.55	2.66×10^{-13}	2.63	5.55×10^{-4}
Wick 3	7.97	2.2	3.23	2.21×10^{-13}	2.65	6.79×10^{-4}

CC at the worst cold case, α is the void fraction of the CC at the worst hot case, V_{vl}, V_{cl}, and V_{ll} are total volumes of the vapor lines, condenser lines, liquid lines, respectively; V_w is the total volume of the wicks, V_{gr} is the total volume of the vapor grooves; $\rho_{l,c}$, $\rho_{v,c}$, $\rho_{l,h}$, and $\rho_{v,h}$ are the densities of liquid in the worst cold case, of vapor in the worst cold case, of liquid in the worst hot case, and of vapor in the worst hot case, respectively; N is the evaporator number, and ε is the wick porosity.

In the experiment, the exact liquid filling volume is 81.2 ml. According to the charge ratio definition:

$$\alpha = V_{liquid}/V_{total} \tag{4}$$

where, V_{liquid} is the volume of the working fluid charged into the system at ambient temperature and V_{loop} is the loop total volume. Therefore, the charge ratio of the system is 69 %.

In order to eliminate the negative effect of NCG, the system should be rarefied before being charged. The absolute pressure of the degassed system was 3.0×10^{-4} Pa.

2.3. Test method

The test system includes ME-LHP prototype, electric heating system, cooling system and data collector system. The electric heating system consists of three metal ceramics heaters with active heater area of 10.1 cm^2 and each heater was measured by a power meter with 0.5 % accuracy. There was a copper sheet between the evaporator heating surface and the metal ceramics heater to ensure close contact and can also uniform the temperature. The cooling system consists of a recirculation chiller with an accuracy of ± 1 °C.

Four thermocouples were set on each of the evaporator heating surface for temperature measurement, and the average temperature of them was adapted as the final temperature of the heating surface. On evaporators own vapor line, three thermocouples were set, six in total, which were respectively located at the outlet of the evaporator and the middle of the vapor line. And the evaporator outlet temperatures took the average value of the temperature measured by the two thermocouples. Both on the inlet and the outlet of the condenser were measured by thermocouples. In the end, three thermocouples were set on the main road of the liquid line, and two thermocouples were set on the separated liquid line to monitor the backflow of the working fluid. The thermocouples mentioned above were all *T*-type thermocouples with ± 0.5 °C accuracy. And data collector "Keithley 2700" was used to record the temperature signals every 3 s.

During the test, the ME-LHP prototype and the heating system were covered with the thermal insulation material(PVC/NBR, Fuerda, thermal conductivity 0.034 W/m·K) to reduce the heat leakage.

2.4. Test procedure

The system condition, such as vapor–liquid distribution before each test, has great influence on the start-up characteristics[22]. Therefore, keeping the same initial condition before the test is important. In the experiment, the system would be kept in the required inclination before each series of tests for more than 12 h. And the condenser would work 30 min before the heat load was applied to evaporators to reach the favorable vapor–liquid distribution. When the successful startup phenomenon was observed and the temperature at each measuring point was stable for 20 min, the heat load would be removed. And the condenser kept working about 30 min to help the system quickly return to the initial condition. Then the next test would be conducted.

3. Results and discussions

3.1. The effects of interactions between evaporators

Because of the multi-branch structure in ME-LHP, the interaction between working and non-working evaporators could be more complex than conventional LHP with just one single evaporator. To explore the interaction mechanism between evaporators on the start-up process, the experiments of single evaporator start-up, double evaporator start-up and all three evaporators start-up were carried out. Then the experimental phenomena were comprehensively analyzed and the mechanisms were also explored.

3.1.1. Start-up characteristic with one individual evaporator

Fig. 4 shows the start-up process of only one evaporator 1(E1) operating, and the heat sink temperature was set at −10 °C. During the test, the evaporators and condenser remained horizontal to avoid gravity's influence. Fig. 4(a) presents the start-up process of E1, with 25

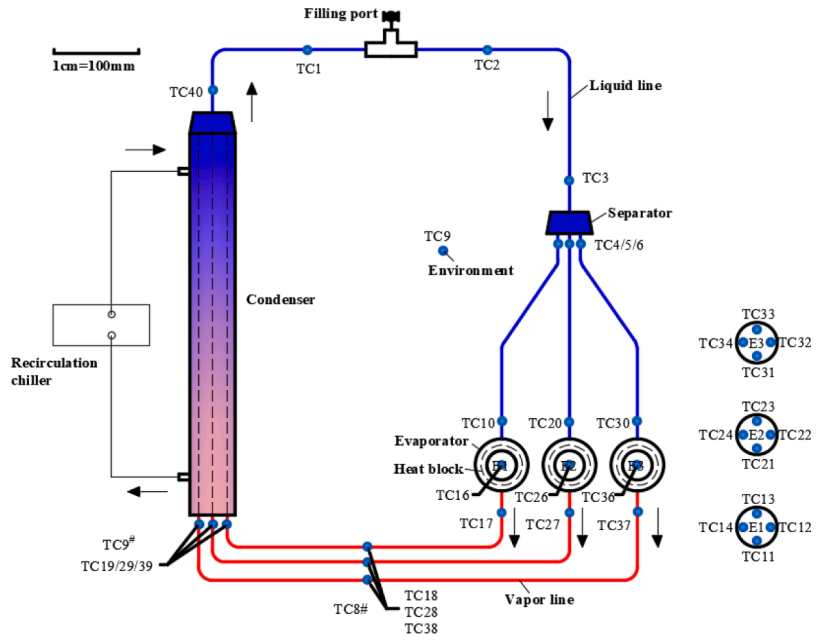

(a) Test schematic of the ME-LHP system.

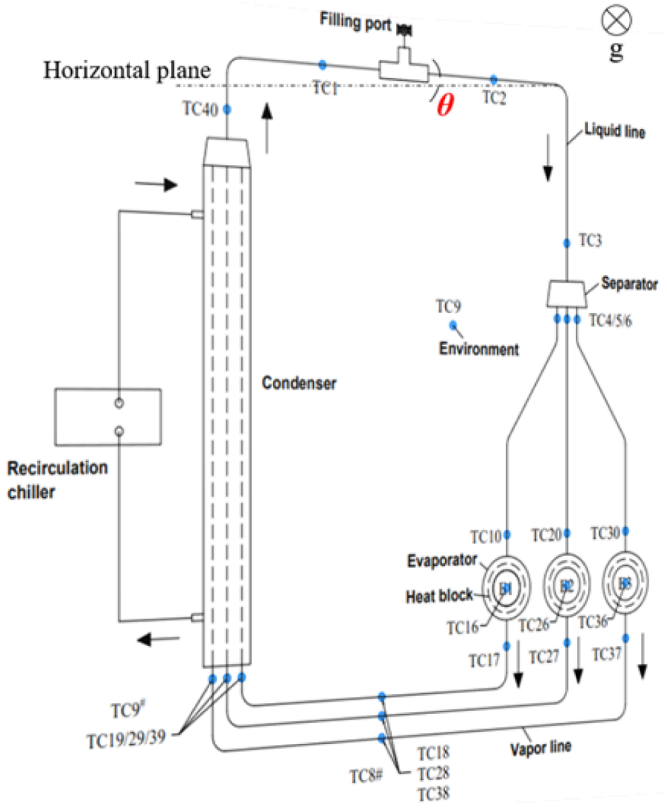

(b) Test schematic of the ME-LHP with gravity-assisted angle.

Fig. 3. System diagram of the flat disk ME-LHP.

Table 2
The main parameters of the loop components.

Components	Dimension	
Evaporator 1/2/3-SUS 316L	Active heated diameter	36 mm
	Overall height	17 mm
Vapor Groove	Wide	2 mm
	Height	2.5 mm
	Number N	10
Vapor chamber	Diameter O./I.	46/41 mm
	Height	5 mm
Compensation chamber 1/2/3-SUS 316L	Diameter O./I.	36.5/34.5 mm
	Height	9 mm
Porous wick-Nickel	Diameter-1/2/3	38.32/38.44/38.78 mm
	Height-1/2/3	1.66/1.46/1.8 mm
	Porosity-1/2/3	72 %/70 %/70 %
Vapor line-SUS 316L	Diameter O./I.	4/2mm
	Length-1/2/3	537/647/757 mm
Liquid line1/2/3-SUS 316L	Diameter O./I.	4/2mm
	Converged length	681 mm
	Separated length-1/2/3	271/252/271 mm
Condenser-SUS 316L	Length	500 mm
	Width	36 mm
	Height	16 mm
Components	Dimension	
Evaporator 1/2/3-SUS 316L	Active heated diameter	36 mm
	Overall height	17 mm
Vapor Groove	Wide	2 mm
	Height	2.5 mm
	Number N	10
Vapor chamber	Diameter O./I.	46/41 mm
	Height	5 mm
Compensation chamber 1/2/3-SUS 316L	Diameter O./I.	36.5/34.5 mm
	Height	9 mm
Porous wick-Nickel	Diameter-1/2/3	38.32/38.44/38.78 mm
	Height-1/2/3	1.66/1.46/1.8 mm
	Porosity-1/2/3	72 %/70 %/70 %
Vapor line-SUS 316L	Diameter O./I.	4/2mm
	Length-1/2/3	537/647/757 mm
Liquid line1/2/3-SUS 316L	Diameter O./I.	4/2mm
	Converged length	681 mm
	Separated length-1/2/3	271/252/271 mm
Condenser-SUS 316L	Length	500 mm
	Width	36 mm
	Height	16 mm

W(2.46 W/cm2) heat load. While the heat load was applied to E1, there was a sharp and quick temperature increase in the heating surface and the evaporator outlet. After about 40 s, the temperatures reached the peak value, 22.7 °C and 19.3 °C, separately. Besides, except for temperature increase, the liquid line and the evaporator inlet temperature decreased from 3 °C to −5 °C and 11 °C to −2 °C separately. The temperature increase of the evaporator outlet and the decrease of the evaporator inlet can be seen as a sign that the circulation of the system was being established. This phenomenon implied that the generated vapor entered the vapor line smoothly and pushed the liquid to circulate in the loop. Temperature overshoot was very obvious at 25 W, which was the typical temperature characteristic in low-power startup. One reason for this phenomenon could be that the establishment of the working fluid circulation was relatively slow in the low-power startup, and the heat leakage to CC raised its temperature quickly. On the other hand, a certain liquid superheat was necessary for evaporation[29]. The temperature overshoot was 10 °C during the startup. Then the loop cycle quickly stabilized under the combined effect of the capillary pressure and phase-change driving force. The start-up time is defined as the time from the heat load applying to the evaporator to a drop appearing in the liquid line temperature[29]. The start-up time was about 89 s.

Fig. 5(b) shows the start-up process of E1 operating under the maximum allowable heat load 75 W(7.37 W/cm^2). The heating surface and evaporator outlet safety temperatures were set below 50 °C and 45 °C when the system operate stably. Compared with 70 °C, which most electric devices can withstand[30], the safety temperatures set in the experiment were much lower than this value. The start-up time under 75 W was significantly reduced compared with the process of 25 W, from 89 s to 65 s. There was no more temperature overshoot starting under 75 W, but a fast and smooth transition to a steady stage. As high heat load applied, the evaporation efficiency was greatly improved and the mass flow rate increased apparently, thus the circulation in the loop could be established quickly. In addition, the reback flow not only provided the working liquid required for evaporation, but also cooled the CC, and annihilated the vapor bubbles generated by the temperature rise in the CC, thus reducing the pressure difference required for circulation and keeping the vapor temperature within an acceptable range, which was beneficial to the start-up process[30]. As a result, further temperature difference between CC and vapor (ie. 10.2 °C) could be seen in this case (2 °C at 25 W). Besides the reasons mentioned above, the existence of multiple branches in the system could be another reason. The amount and rate of the working fluid cycle increased with the increase in heat load. Thus more working fluid was involved in the cycle. Fig. 5 shows the start-up process of E2 and E3 under 75 W heat load, in which the characteristics were similar to E1. But in Fig. 5(b), the temperature of E1

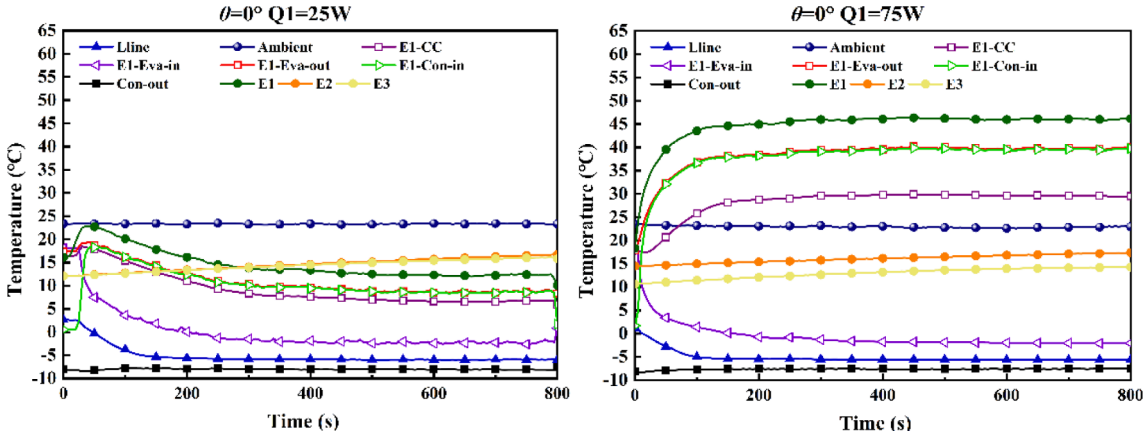

(a) Q = 25 W (b) Q = 75 W

Fig. 4. Start-up process of E1 under 25 W and 75 W at −10 °C heat sink temperature.

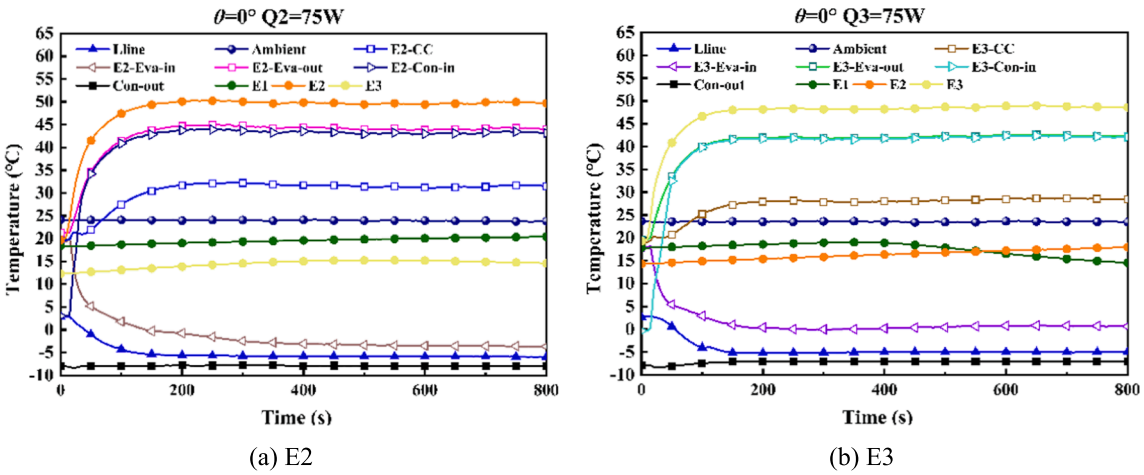

(a) E2 (b) E3

Fig. 5. The temperature characteristics of E1 when E3 was applied 75 W with heat sink temperature of −10 °C.

heating surface decreased when E3 operated under 75 W. The temperature characteristics of E1 when E3 was applied 75 W was shown in Fig. 6, there was something interesting happening in E1. During the startup process of E3, the temperature of E1 vapor line, E1 evaporator outlet and E1 heating surface decreased in turn. And the E1 condenser-inlet temperature was the lowest, followed by the E1 vapor line, and the temperature of E1 heating surface was the highest. The reason for this phenomenon could be that there was only one evaporator working, a large number of the working fluid remain in the non-working branch in the liquid phase. When E3 started working, the working fluid began to circulate, and the condensed working fluid converged at the mixer which was in the end of the condenser, forming a liquid disturbance in the mixer, thus causing the reverse flow from the condenser to E1. Therefore, the temperature of E1 condenser-inlet was the lowest, because this was the outlet of the backflow, and the temperature rose gradually along the vapor line due to the heat leakage with the environment. The flow inside the mixer is shown in Fig. 7. This reverse flow phenomenon could be observed in any working condition when E3 operated alone. But no similar phenomenon was observed during the startup of other evaporators, the reason may be the asymmetry of the positions of the three evaporators.

During the single evaporator start-up process, the characteristics of no-working evaporators were also worth noting. Fig. 8 shows the temperature variations of the evaporator outlet, inlet and CC in no-working evaporators(E2,E3), when E1 operated by itself under heat load 75 W

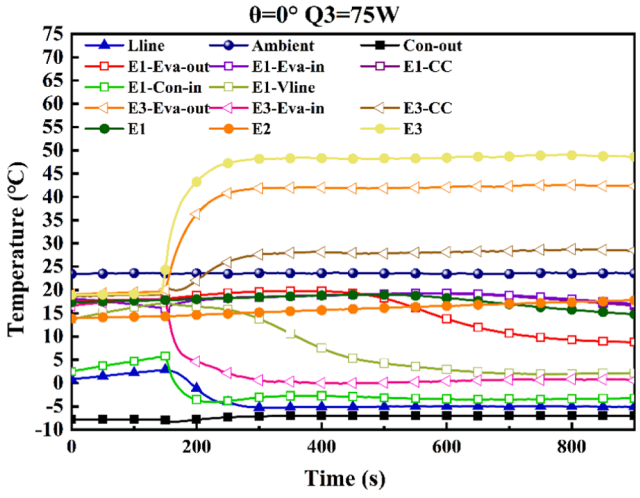

Fig. 6. The temperature characteristics of E1 when E3 was applied 75 W with heat sink temperature of −10 °C.

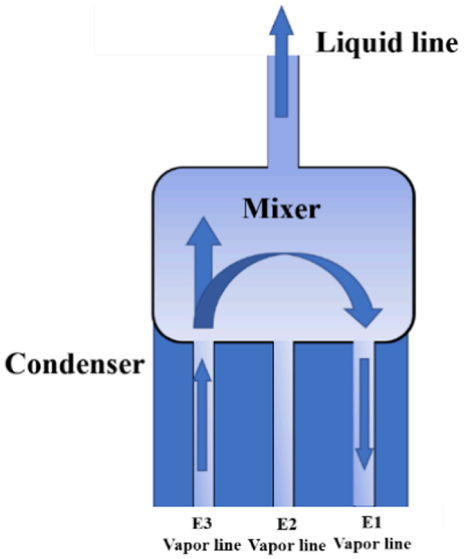

Fig. 7. The flow inside the mixer when E3 operated alone.

(7.43 W/cm^2). It can be seen from the figures that during E1 startup, the temperature of each characteristic point of E2 and E3 remained almost stable, the small rise in temperature could be explained by the heat exchange between the evaporator shell and the environment. This meant that unlike other tests [1,22], when E1 started alone, the vapor generated by it could not enter the non-working evaporators(E2,E3), but went directly to the condenser to establish single-branch cycle and there was no evaporator or CC working as a condenser due to the separated vapor line equipped on the evaporator.

Due to the volume limitation of the flat plate evaporator, the distance between CC and heating surface was rather short compared with the cylindrical evaporator and the contact area between the wick and the evaporator shell was also smaller, thus the vapor getting into the non-working evaporators would reduce the operating performance of the system. The heat-sharing model in cylindrical evaporator ME-LHP was not quite suitable for flat disk ME-LHP. Therefore, evaporators equipped with their own vapor line were proposed in the new design. But there still retained communication between evaporators, the convergence point was set at the condenser outlet which connects the CC, and this will be discussed in detail in section 3.1.2 when multiple evaporators were started.

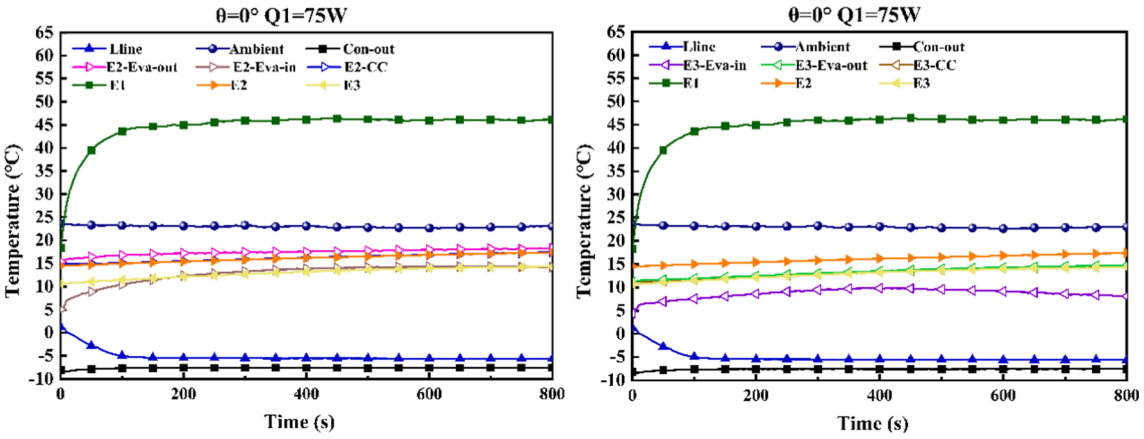

(a) E2 (b) E3

Fig. 8. The temperature characteristics of E2 and E3 when E1 was applied 75 W with heat sink temperature of −10 °C.

3.1.2. Start-up characteristic with multiple evaporators

Fig. 9 shows the start-up process for any two evaporators in the ME-LHP at even heat load(7.43 W/cm^2) with 2° gravity-assisted angle at heat sink −10 °C, and the heat load matrix can be seen in Table 3. As Fig. 9 shown, the relative position between the two working evaporators had little effect on the starting characteristics, so the starting processes of these three cases almost remained the same.

Case 1 was taken as an example to illustrate this process. With the application of thermal load, the heating surface temperatures of E2 and E3 increased rapidly as shown in Fig. 9(a). Phase change occurred in the evaporators, as temperature raised. Then the generated vapor escaped from the vapor channel into vapor lines, increasing the temperatures of

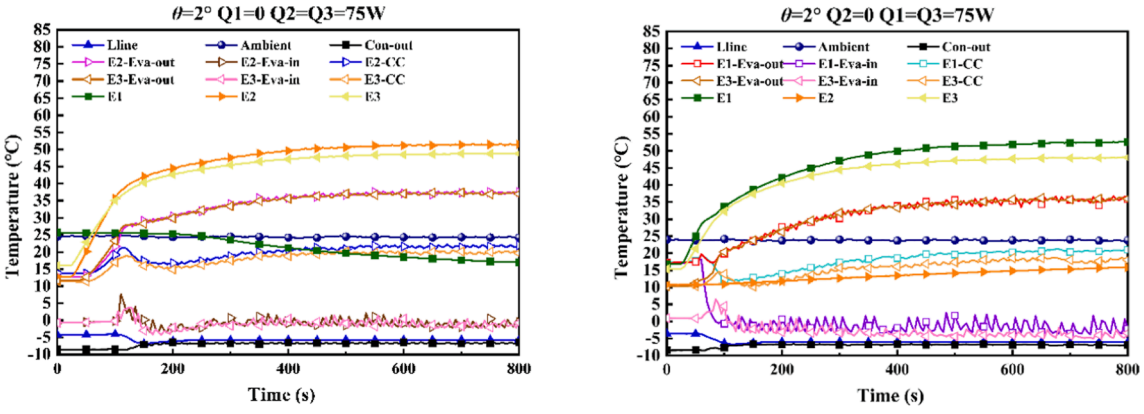

(a) the start-up process of case 1. (b) the start-up process of case 2.

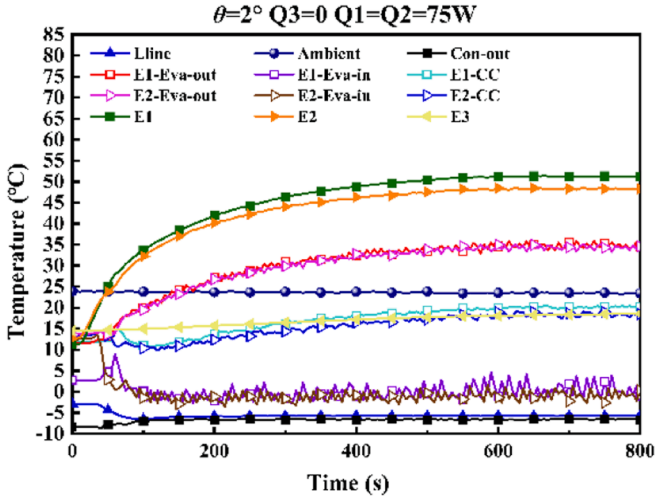

(c) the start-up process of case 3.

Fig. 9. Start-up process for any two evaporators under equal heat loads with heat sink temperature of −10 °C.

Table 3
Heat load matrix for any two evaporators started.

Situation	E1 Heat Load/W	E2 Heat Load/W	E3 Heat Load/W
Case 1	0	75	75
Case 2	75	0	75
Case 3	75	75	0

the E2 and E3 outlets. At the same time, the temperature of the liquid pipeline decreased from −3 °C to about −5 °C, which meant the liquid accumulated in the condenser was pushed into the liquid line. It was noted that the CC temperature curve had a process of rising first and then falling. The rising trend could be caused by the heat leak from the evaporator, and then the upward trend was restrained as the supercooled reflux entered the CC. In case 1, the peak value of CC2 and CC3 reached 20.9 °C and 18.6 °C respectively, and finally stabilized at about 19 °C and 17 °C respectively. The total start-up time required for both evaporators was the same, about 120 s.

Although the two evaporators were under the same heat load, it could be seen that the heating surface and CC temperatures of them were different, as shown in Fig. 10. The CC with the highest temperature controlled the operating temperature, while the higher the temperature of the CC, the higher the temperature of the heating surface. The temperature of CC was mainly affected by two factors, one is the reflux liquid mass from the condenser and the other was the heat leak from heating surface. When the same heat load was applied, the difference of the reflux liquid could be the main reason for the temperature difference of the CC. The existence of the gravity-assisted angel made E3 in an advantageous position in liquid supply compared with the other two evaporators. Therefore, in case 1 and case 2, the temperatures of E3 CC and heating surface were the lowest. When only E1 and E2 were started, the liquid supply of E2 was better than E1 due to the same reason, so that the temperature of E2 CC and heating surface was lower than E1. From what had been mentioned above, the liquid distribution was the reason for the different performances of evaporators.

The effect of returning liquid on the system performance could be verified when all the three evaporators simultaneous started. With 2° gravity-assisted angle, the three evaporators were applied an equal thermal load of 65 W(6.44 W/cm^2), and the startup process showed in Fig. 11. When all three evaporators worked, E3 CC still kept the lowest temperature and remained at 24 °C after stabilization. And the temperature difference between E2 heating surface and that of E3 was tiny, the two temperatures curves were almost coincided. This was due to the start-up of E1 and E3, which jointly strengthened the liquid supply of E2, so that the E2 heating surface temperature could maintain at a low level.

In addition, the average value of evaporator inlet temperature of E1 was the highest, about 0 °C. The temperature fluctuation range was also the largest, and the difference was up to 6.2 °C. Besides, the temperature fluctuation showed a certain regularity, large amplitude fluctuation and small amplitude vibration occurred alternately. The reason for this phenomenon was that when the three evaporators worked at the same time, the demand for working fluid of the three evaporators formed a competitive relationship with each other. E2 and E3 were in an advantageous position in liquid supply due to the assistance of gravity angle.

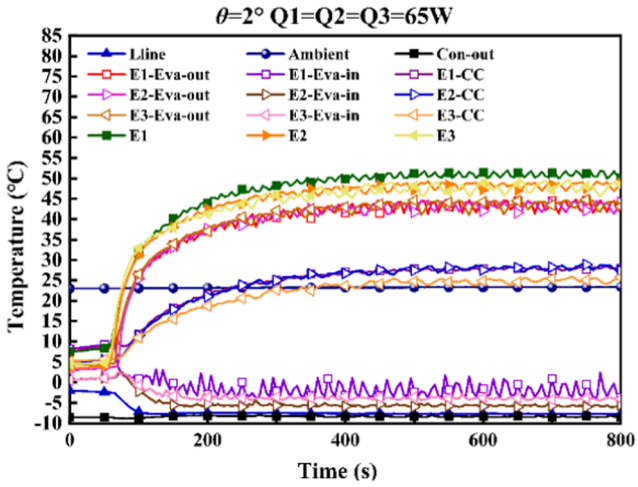

Fig. 11. Startup characteristics of ME-LHP when all three evaporators were heated at the heat sink at −10 °C.

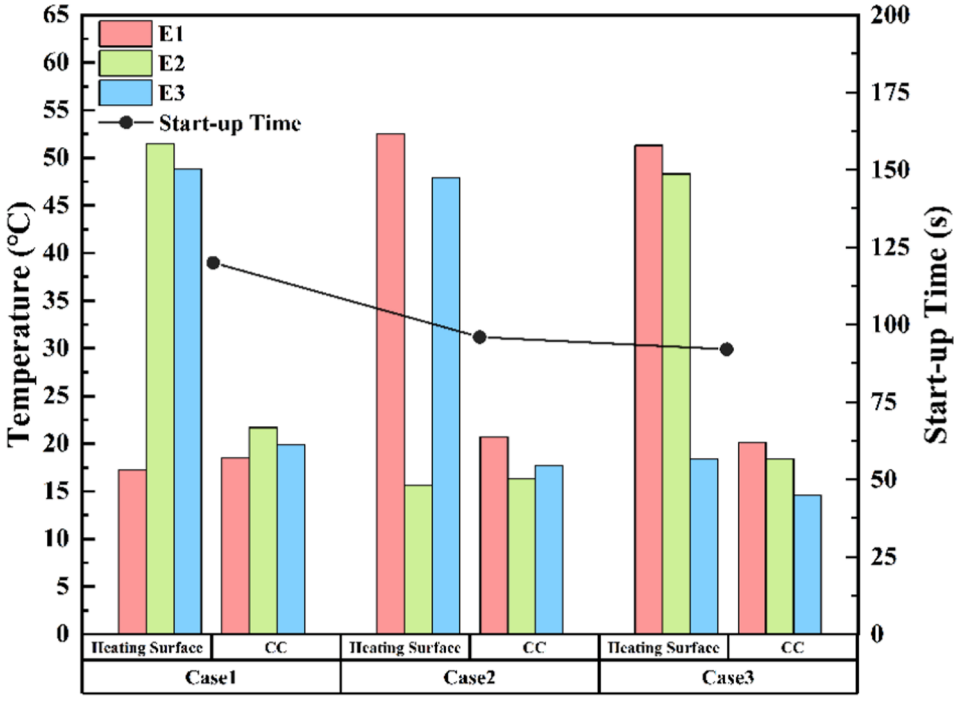

Fig. 10. Stable temperature of ME-LHP when any two evaporators under equal heat loads.

During the operation, when returning liquid flowing to E2 and E3 was insufficient, the liquid supply of E1 would be in a state of shortage, and its inlet temperature fluctuated greatly. At then, there was a large amount of returning liquid accumulated in E2 and E3 and the demand for returning liquid decreased, at this time, the liquid supply of E1 was improved and the fluctuation range of inlet temperature was reduced. Therefore, in ME-LHP, due to the competition of reflux liquid, the high filling ratio can be the solution to ensure sufficient supply of returning liquid when multiple evaporators work at the same time.

3.2. The effects of the heat load distribution

In order to explore the influence of heat load distribution on the start-up process, different heat loads were applied to evaporators. And the experimental results were illustrated and analyzed. In the experiment, the heat sink temperature was kept at −10 °C and the gravity-assisted angle was 2°.

3.2.1. Unequal heat load start-up of dual evaporator

Fig. 12 shows the start-up process when the two evaporators were started with unequal heat load while keeping the left evaporator unstarted. The heat load matrix can be seen in Table 4.

Case 1 was taken as an example. It can be seen from Fig. 12(a) that although E1. and E2 were in different heat load conditions(the power difference between them was about 40 W), when the system reached the steady state, the outlet temperature of these two evaporators remained the same, both maintained at about 25 °C and fluctuated slightly. This phenomenon was the result of the communication between the liquid lines. The vapor generated by each evaporator was condensed through the condenser and then the supercooled liquid converged. In the CC of each evaporator, pressure communication was formed through the liquid separator, and the liquid only worked as a pressure-transfer medium. That means, as long as each branch was in the liquid phase at the converging point, the steam pressure required by each branch would be the same. So that the outlet temperature of each evaporator would always remain the same, regardless of the heat loads were the same or unequal.

Table 4
Unequal heat load matrix for any two evaporators started.

Situation	E1 Heat Load/W	E2 Heat Load/W	E3 Heat Load/W
Case 1	75	35	0
Case 2	35	0	75
Case 3	0	75	35

The unworking E3 was not affected by E1 and E2. The outlet temperature of E3 kept rising slowly and uniformly from the initial temperature of 10 °C. The temperature change of E3 could be explained by the heat exchange between the system and the environment.

The temperature of E1 and E2 inlet remained the same (-5 °C in steady-stage), while the outlet temperature kept the same. The heating surface temperature of E1 was significantly higher than that of E2. The stable temperatures were 42.7 °C and 34.0 °C respectively, and the temperature difference was about 8 °C. This phenomenon was corresponded to the difference of heat loads.

However, the temperature of the CCs showed a difference in heat load distribution. The E1 CC temperature under high heat load was lower than that of E2, which were 13.9 °C and 17.5 °C respectively, with a temperature difference of about 4 °C. The reason for this phenomenon could be that, under high heat load the phase change rate was much

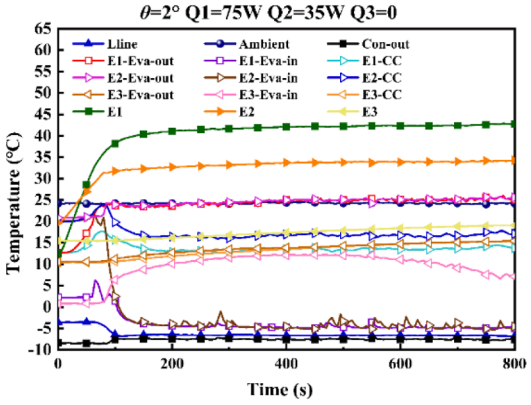

(a) the start-up process of case 1.

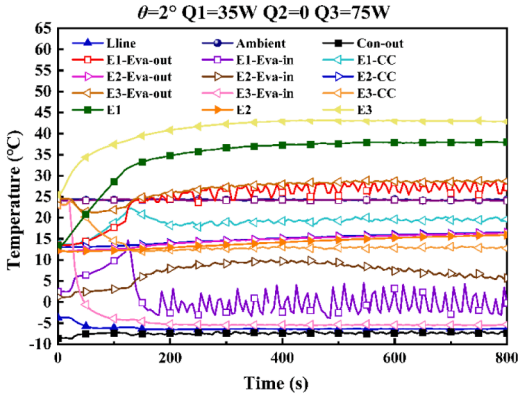

(b) the start-up process of case 2.

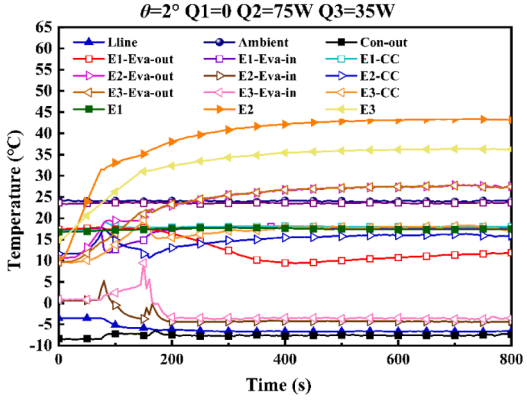

(c) the start-up process of case 3.

Fig. 12. Start-up process for any two evaporators under unequal heat loads with heat sink temperature of −10 °C.

higher, resulting in the faster circulation rate of the working fluid in this branch. The generated vapor was quickly pushed into the vapor line, increasing the pressure difference on the wick, which was beneficial to the liquid supply of the CC, and more reflux liquid entered the CC under a higher heat load. Therefore, in case 1, the temperature of E2 CC was lower than E1 CC, even if the thermal load applied E2 was higher than E1. In the other two cases, the same phenomenon also existed, as shown in Fig. 13. While the evaporator applied a higher heat load, the CC temperature would be lower than the other one.

What should be addressed is that, the influence of gravity on the system can also be observed. Compared Fig. 13(a) with Fig. 13(b), though E1 and E2 worked under the same load, the temperature of E2 CC was lower than that of E1 CC and the temperature difference was about 3 °C. The reason for this phenomenon was the quantity difference of the returning fluid caused by the different liquid distribution. Because E2 was at the advantageous potion under the gravity-assisted angle, more liquid would flow back to its CC than E1. In section 3.3 the gravity influence on the system was investigated and analyzed.

3.2.2. *Unequal heat-load startup of triple evaporators*

Fig. 14 shows the start-up process when the three evaporators applied different power, and the heat loads distribution matrix is shown in the Table 5. It was highly consistent with the unequal start-up process of dual evaporators. When triple evaporators applied different heat loads, the vapor temperature of each branch also remained the same. In addition, the vapor temperature was not determined by the branch bearing the highest heat load. Fig. 15 shows the start-up process of E2 operating alone at 65 W. The E2 outlet temperature has reached about 41 °C. But when triple evaporators started with unequal heat loads, the vapor temperature was just 24.8 °C in a steady state. The temperature difference was about 16.2 °C, which means that when the three evaporators started at the same time, the outlet temperature would approach an intermediate temperature, which was lower than that in the single one started alone. Compared with E2 started alone, the heating surface temperature of E2 was also lower when all evaporators participated in. The temperature difference was close to 5 °C in two start-up conditions. This means that triple evaporators worked together under unequal heat loads, improving each branch's heat transfer capacity and even the whole system's capacity.

There were two reasons for this phenomenon. Firstly, compared with the single evaporator working, all the working liquid inner the system participated in the circulation. On the one hand, the increasing working fluid reflux replenished the working fluid and maintained the wick's liquid supply. On the other hand, the supercooled reflux liquid could cool the CC, annihilate the bubbles generated inside, weaken the subcooled flow boiling and reduce the vapor volume inside CC[27]. Secondly, heat loads distribution could co-operate with liquid distribution. Compared with the three evaporators simultaneous started under equal heat loads(65 W), it can be seen that the E1 inlet temperature fluctuates more, which means that there was a large shortage of liquid supply for E1. However, because the heat load applied to E1 was not high in this way of starting, the liquid supply was enough to meet its phase change demand even it was at a disadvantageous position in liquid supply. On the opposite, E2 bearing higher heat load got more reflux working fluid. In this situation, the liquid distribution was more reasonable.

The temperature of the CC bearing the highest thermal load was lower than that of the other two CCs, as shown in Fig. 16. To a certain extent, the temperature of CC could reflect the supply of the reback flow to each branch. The CC with low temperature suggested that the return flow of the branch was sufficient, so the CC could be cooled at instant. High heat load increased the rate of phase transition rate, and the demand for working liquid also increased. In addition, the existence of liquid separator kept the distribution of liquid in a self-adapted way. The liquid separator served as a liquid container to store the returning fluid before the evaporator. Affected by the difference in heat loads, the required quantity of returning liquid is not equal for each branch, then the liquid stored inside the separator would enter the different branches at the quantity as required. Therefore, more liquid flowed backed to the high heat load branch, making the CC temperature in at a low level.

It was because the positions of the evaporator were not the same, they were in advantageous or inferior in liquid distribution. Combined with the experimental results, it was considered that there was an optimal heat load distribution for the start-up of ME-LHP under unequal heat load. Taking this system as an example, applying high heat loads to the evaporator in advantage positions and low heat load to the evaporator in disadvantage positions was conducive to the start-up of ME-LHP

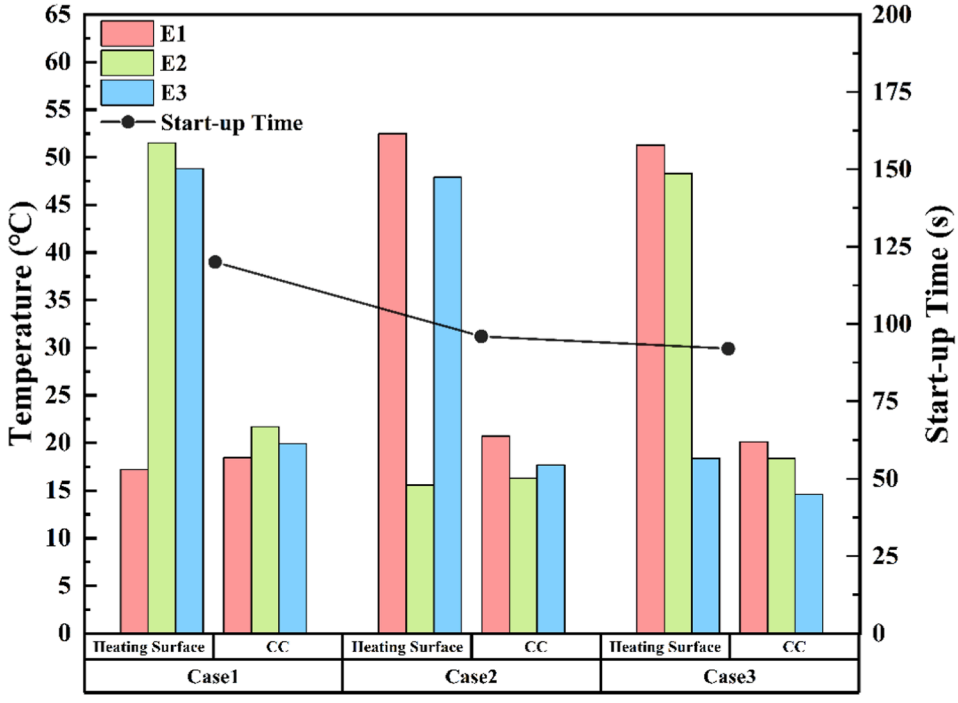

Fig. 13. Stable temperature of ME-LHP when any two evaporators under unequal heat loads.

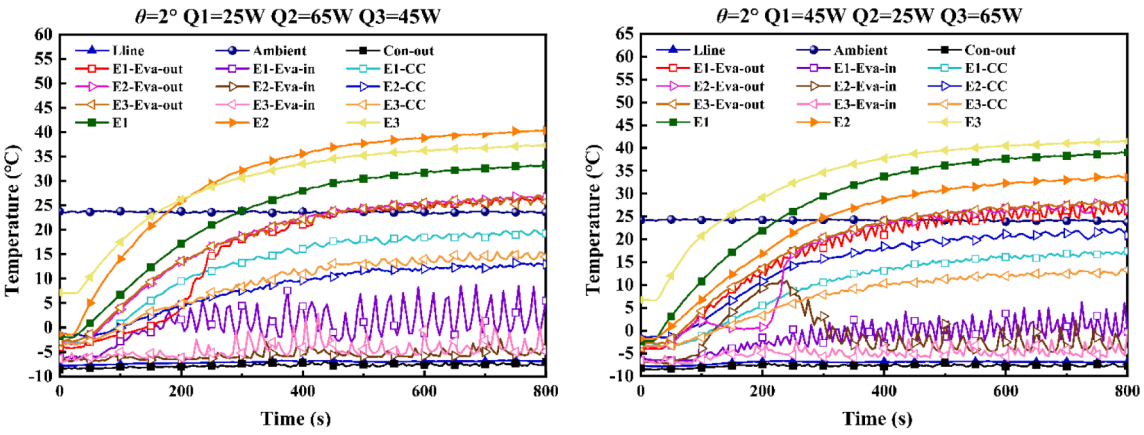

(a) the start-up process of case 1.

(b) the start-up process of case 2.

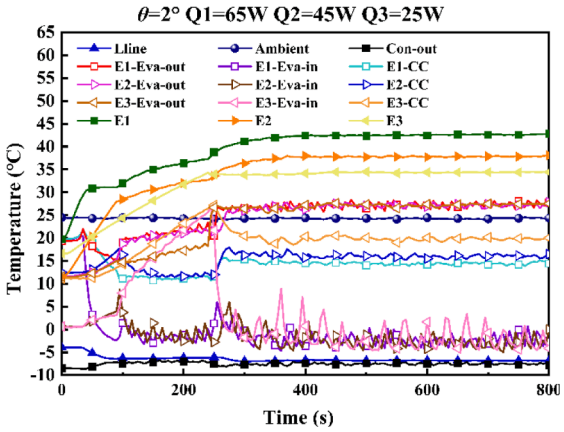

(c) the start-up process of case 3.

Fig. 14. Start-up process for three evaporators under unequal heat loads with heat sink temperature of −10 °C.

Table 5
Unequal heat load matrix for all three evaporators started.

Situation	E1 Heat Load/W	E2 Heat Load/W	E3 Heat Load/W
Case 1	25	65	45
Case 2	45	25	65
Case 3	65	45	25

and therefore can improve the heat transfer capacity.

3.2.3. The pressure and temperature of the working fluid inside ME-LHP during the operation

Compared with the traditional single evaporator LHP, the thermodynamic process inside the ME-LHP system is more complicated. In order to illustrate the thermodynamic state of the working fluid when the system operates, the *P-T* diagram is provided in this section, as shown in Fig. 17(b).

Due to the difference of heat load applied in each evaporator, the difference of the wick and the asymmetric arrangement of the pipeline, the *P-T* curve of each evaporator is different. When started under different heat loads, the saturation points of each evaporator(E1,E2 and E3) are in different positions at the saturation curve. Then the generated vapor is further heated by the heating surface and gets into the evaporator outlet (17,27,37). Because of the influence of the liquid convergence, the vapor pressure and temperature become the same. The superheated vapor continues to flow along the vapor line, and the

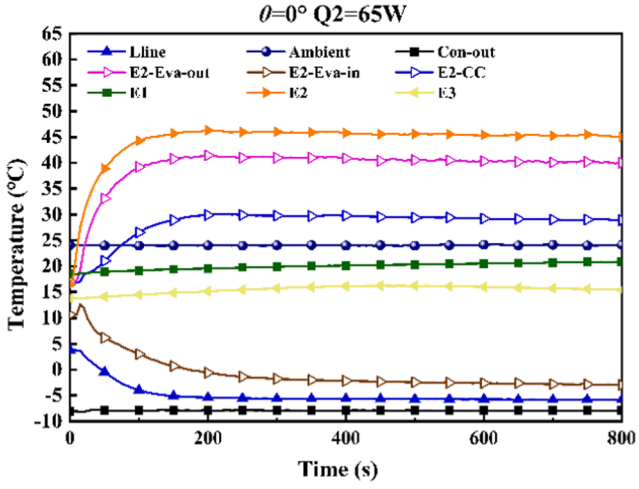

Fig. 15. Start-up process of E2 worked alone at 65 W at heat sink temperature of −10 °C.

pressure continues to decrease. At the same time, because of the heat leakage from the vapor line to the environment, the temperature of the vapor also decreases and then the vapor gets into the condenser (19, 29, 39). Inside the condenser, the superheated vapor goes through three processes, the superheated section process, the two-phase section

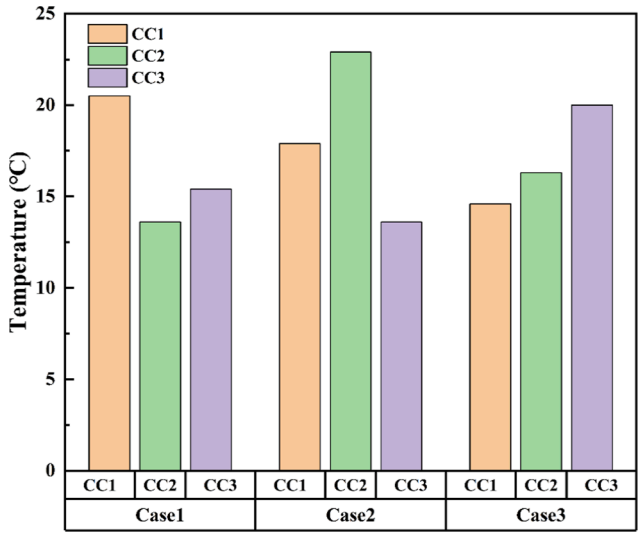

Fig. 16. The CC Startup characteristics of ME-LHP when three evaporators were under unequal heat load distributions.

process, and the supercooling section process. Then the supercooled liquid flows into the liquid line, where the pressure decreases due to the influence of flow resistance and the temperature increases caused by the heat leakage. At the separator, the supercooled liquid is divided into different liquid lines. Because of the difference of the liquid line and evaporator state, the saturation states of the working fluid after entering each compensation chamber (16, 26, 36) are different. Then the working fluid flows through the wick with high-pressure loss and temperature increase caused by the heating surface(E1,E2 and E3). The cycle of this process ensures the stable operation of ME-LHP.

3.3. The effect of the gravitational head

In ground applications, the gravity field will have a non-negligible effect on the ME-LHP start-up process. Due to the existence of multiple branches, the liquid needs to be distributed through the liquid separator. The gravitational head will greatly affect the distribution of reflux liquid and the vapor/liquid distribution inside the system, thus affecting the start-up of the system. In order to explore the influence of gravity on the start-up of ME-LHP, the start-up experiments were carried out under the gravity-assisted angle. At the same time, in order to fit the actual engineering application in high-integrated scenarios, only small gravity-assisted inclination angles were selected during the experiment (2°, 5° and 10°). Fig. 18. shows the schematic of the ME-LHP system in gravity-assisted inclination by side view.

Fig. 19(a), (b), and (c) shows the start-up process at gravity tilt angles of 2°, 5° and 10°, respectively, when triple evaporators were started with equal thermal load (55 W/5.45 W/cm^2). Under the same gravity-assisted angle, the start-up process of each evaporator remained the same, and there was no temperature overshoot in all cases. In addition, the vapor temperature of each branch remained the same in every working case, and did not change with different gravity tilt angles. This was because the change of gravity-assisted inclination angle did not interfere with the communication between compensation chambers and liquid pipelines.

However, due to the change of gravity-assisted angle, the gravitational head and liquid distribution in every case were different, which could affect the starting characteristics. With the increase of gravity-assisted angle, the fluctuation amplitude of E1 inlet temperature decreased. At the same time, the stable temperature of CC1 decreased successively when the gravity-assisted inclination angle was 2°, 5° and 10° respectively (ig. Only take E1 for example, other evaporators also have the same law). The reason for the above phenomenon was that the increase of gravity-assisted angle auxiliary the reflux liquid reback to the evaporator. Taking the starting process of E1 as an example, the influence of gravity on the system could be divided into two stages. When the angle was small, the effect of assisted liquid reflux was not obvious compared with that of changing liquid separation. This could be called as the dominant stage of liquid separation effect. As for the system structure, the small angle could worsen the liquid distribution of E1, so that more liquid was distributed to E2 and E3.But with the gradual increase of the angle, the effect of gravity on the auxiliary reflux liquid increased gradually. At this time, the auxiliary reflux effect dominated the startup of the system. Therefore, the inlet temperature fluctuation of the evaporator was enhanced. At the same time, due to the increase of liquid return, the CC of each evaporator was effectively cooled, so the stable temperature decreased.

Because the gravity-assisted angle increased the return flow and reflux rate of liquid, the circulation could be established quickly, the start-up time was shortened and the stable temperature was also reduced as shown in Table 6. At the same time, within the set safe temperature range, the heat transfer performance of the system had also been greatly improved. When the gravity inclination angle was 10°, the highest performance was improved by 77 % at the gravity-assisted tilt of $\theta = 10°$than that of $\theta = 2°$, and the peak load could reach 300 W, as shown in Fig. 19(d).

It is noted that when all three evaporators started under the gravity-assisted inclination, the temperature of each measuring point fluctuates significantly. This is due to the instability of the vapor–liquid interface inside the condenser. At the same time, due to the existence of gravity-assisted angle, the return liquid of each branch is distributed unevenly, resulting in the unstable rate of vapor produced by the evaporator, which further aggravates the instability of the vapor–liquid interface and brings about temperature oscillation.

3.4. Thermal resistance and uncertainty analysis

Thermal resistance is always regarded as an important parameter of LHP, which reflects the heat dissipation ability. The thermal resistance of the LHP system(R_{LHP}) is defined as:

$$R_{LHP} = \frac{T_{eva} - T_{cond}}{Q} \tag{5}$$

Where, T_{eva} is the temperature of the evaporator wall, T_{cond} is the average temperature of the condenser which is the average inlet temperature and outlet temperature of the condenser, and Q is the heat load. The variation of R_{LHP} with heat load from 25 W to 65 W with −10 °C sink temperature when three evaporators started at the equal heat load is shown in Fig. 20. With the heat load increasing, the total thermal resistance of three branches was decreased at the same time. But compared with the traditional single-one evaporator LHP, the total resistance of the loop was higher. The high thermal resistance of the system might be caused by the convergence and the separation of the working fluid in the system.

The thermal resistance of evaporator(R_{eva}) is defined as:

$$R_{eva} = \frac{T_{eva} - T_{eva\_out}}{Q} \tag{6}$$

Where, T_{eva} is the temperature of the evaporator wall, $T_{eeva\text{-}out}$ is the outlet temperature of the evaporator, and Q is the heat load. Fig. 21 shows the variation of R_{eva} with heat load from 25 W to 65 W with −10 °C sink temperature when three evaporators started at the equal heat load. The contact thermal resistances are large parts of the evaporator thermal resistance, which should be controlled at a low level. Some methods such as applying high thermal conductive filled silicone between the evaporator and the heating source were obtained during the tests. Through the measures, the evaporator thermal resistance of all three evaporators were kept at a low level during the experiment. The

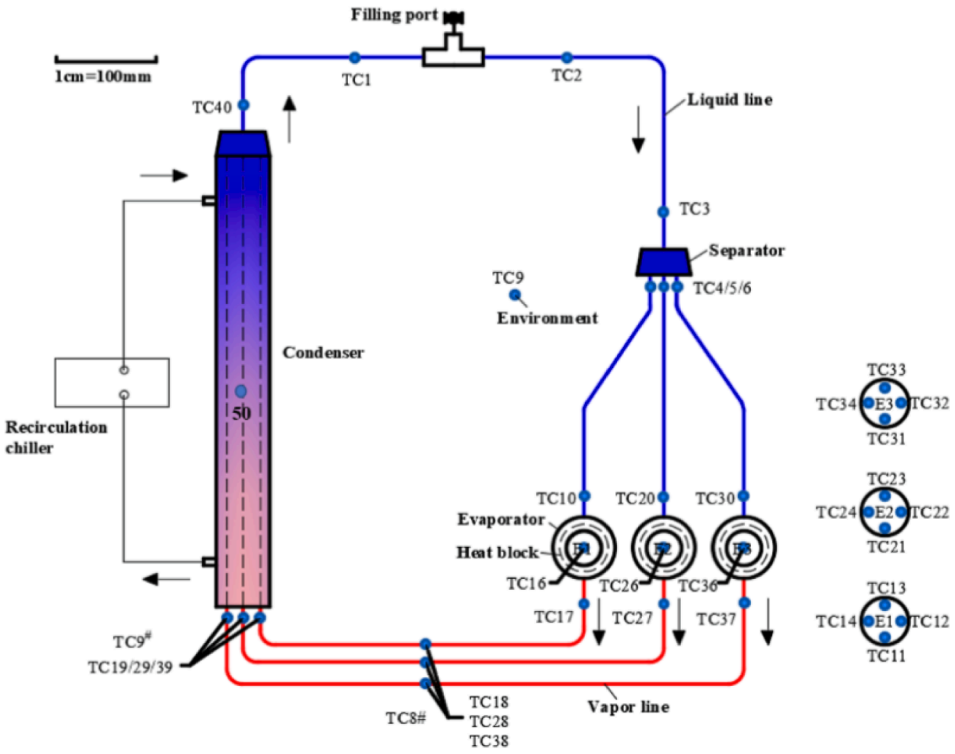

(a) The schematic diagram of the MT-LHP.

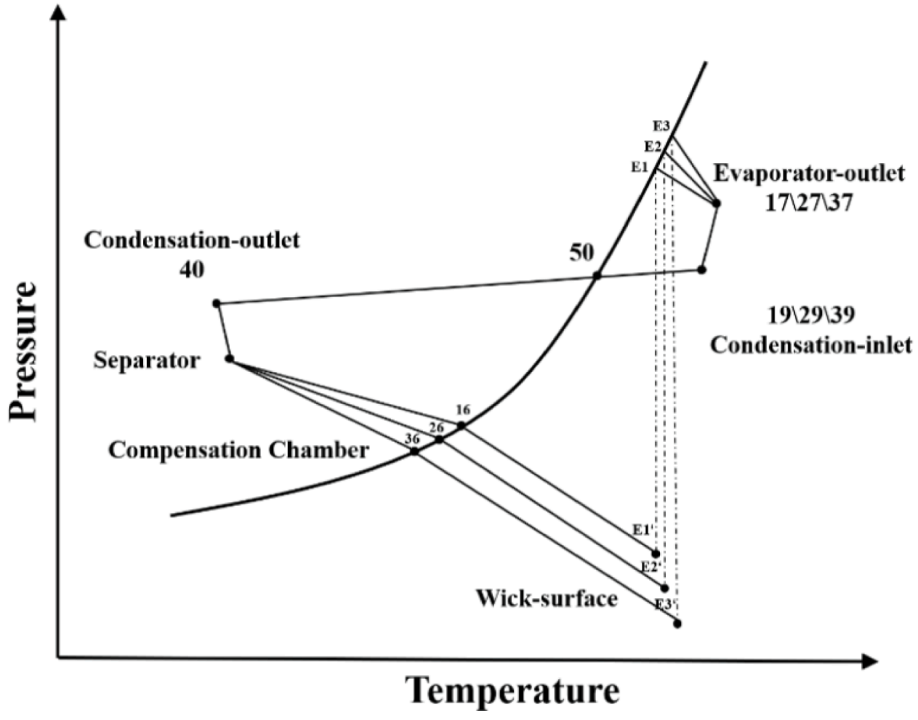

(b) The P-T diagram of the ME-LHP.

Fig. 17. The schematic and P-T diagram of LHP.

difference of three evaporators' thermal resistance was small, which means the heat dissipation capacity difference of the three evaporators in the system caused by the asymmetric structure was small.

The uncertainty of R_{LHP} can be calculated by

$$\frac{\delta R_{LHP}}{R_{LHP}} = \sqrt{\left(\frac{\delta y}{y}\right)^2 + \left(\frac{\delta Q}{Q}\right)^2} \tag{7}$$

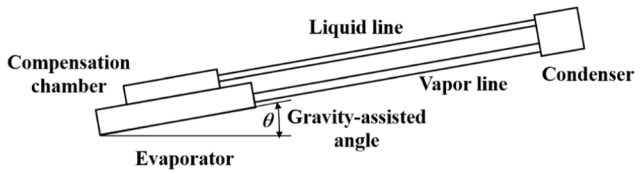

Fig. 18. Schematic of the ME-LHP system under gravity-assisted inclination by side view.

$$\delta y = \sqrt{\sum_{i=1}^{4}\left(\frac{1}{4}\delta T_{eva,i}\right)^2 + \sum_{i=1}^{2}\left(\frac{1}{2}\delta T_{c,i}\right)} \tag{8}$$

$$y = T_{eva} - T_c \tag{9}$$

Where $T_{eva,i}$ is the temperature at heater surface measured by four thermocouples and $T_{c,i}$ is the temperature at condenser inlet and outlet. Due to the accuracy of *T*-type thermocouples were ± 0.5 °C, $\delta T_{eva,i}$ and $\delta T_{c,i}$ were all equal to 0.5 °C. The accuracy of the power meter was 0.5 %. As a consequence, the maximum uncertainty of the E1 R_{LHP}, E2 R_{LHP}, and E3 R_{LHP} were calculated to 3.63 %, 3.01 %, and 2.64 % respectively. The minimum uncertainty were 1.48 %, 1.44 %, and 1.48 % respectively.

4. Conclusion

This paper proposed a novel stainless steel-ammonia ME-LHP system with three flat disk evaporators equipped with their own vapor lines arrangement. The effects of the interaction between evaporators, the heat load distribution, and the gravity-assist angle on the startup behavior of ME-LHP were experimentally studied. The results presented that the new type of ME-LHP showed excellent running performance under different working conditions, which may promote the application of LHP in solving multi-heat sources. The main conclusion can be summarized as follows:

(1) Due to the novel structure of the ME-LHP, with evaporators equipped with separate vapor lines, the adverse impact between evaporators was greatly reduced. And the system still operated stably when only one or two evaporators were involved, which proved the feasibility of the new design.
(2) The performance was improved as the involved evaporators increased. This could be explained by the rising mass of working fluid contained in the cycle. When the number of operating evaporators increased, the liquid accumulating in the non-working branches would be mobilized to establish the cycle.
(3) At the unequal heat load working condition, the ME-LHP obtained the optimal startup performance when high heat load was

Table 6
The temperature of E1 evaporator inlet, CC and the start-up time of ME-LHP under three different gravity-assisted angles.

Temperature	2° Inclination	5° Inclination	10° Inclination
E1 inlet/°C	−1	−0.2	−1.5
E1 CC/°C	19.9	12.6	7.18
Start-up time/s	90	55	40

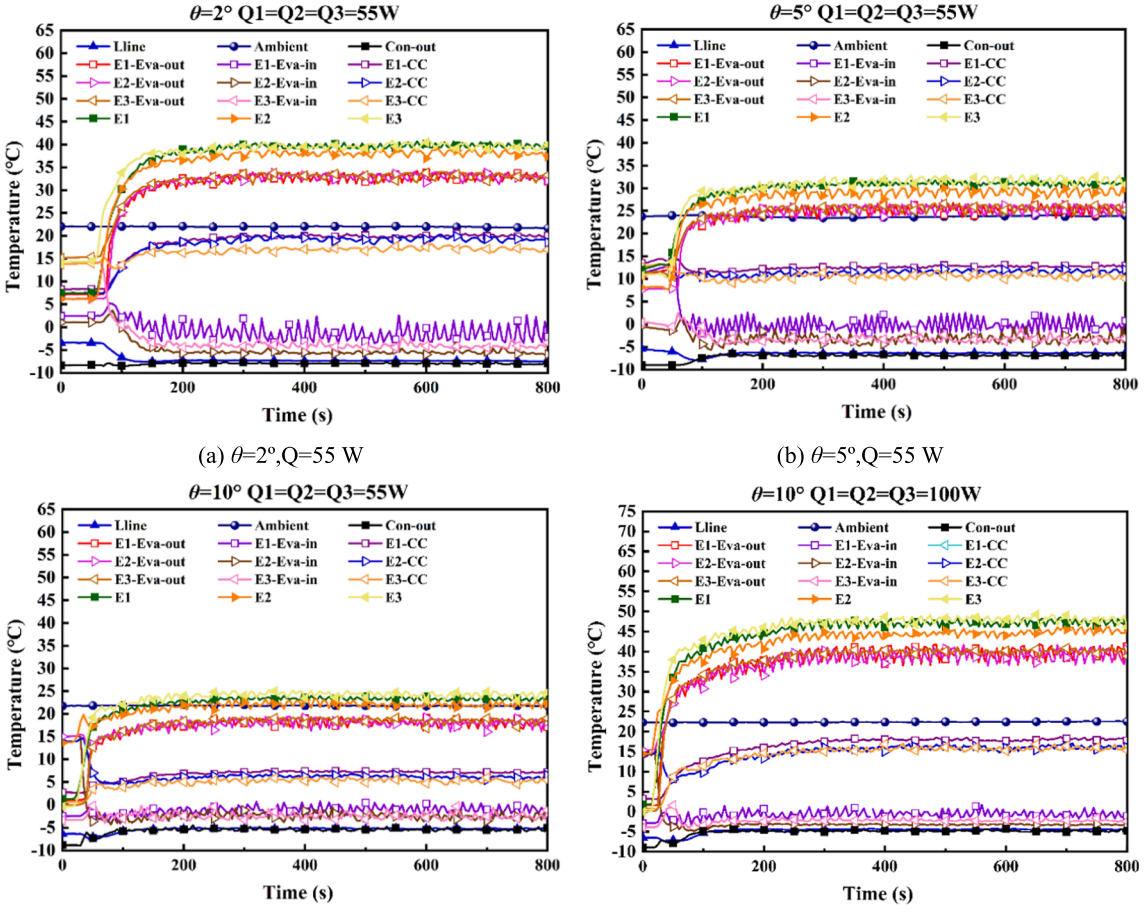

(a) θ=2°,Q=55 W (b) θ=5°,Q=55 W

(c) θ=10°,Q=55 W (d) θ=10°,Q=55 W

Fig. 19. Start-up process for different gravity-assisted angle under equal heat loads with heat sink temperature of −10 °C.

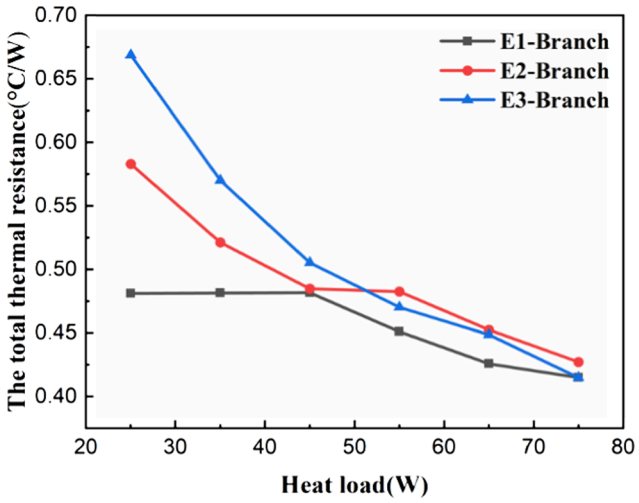

Fig. 20. The R_{LHP} of three branches when three evaporators started with equal heat load.

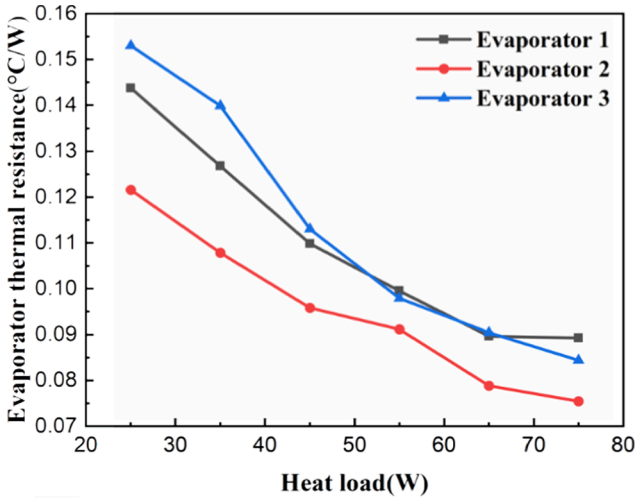

Fig. 21. The R_{eva} of three branches when three evaporators started with equal heat load.

applied on evaporators with the superior position in liquid separation. Besides, the outlet temperature of all evaporators tended to be consistent, even if multiple evaporators worked under unequal heat loads.

(4) The gravity-assisted angle affected the start-up process by changing the non-uniformity of liquid distribution, resulting in different operating performances of every evaporator when working under equal heat loads. The highest performance was improved by 77 % at the gravity-assisted tilt of $\theta = 10°$than that of $\theta = 2°$, and the peak load could reach 300 W.

Declaration of Competing Interest

The authors declare that they have no known competing financial interests or personal relationships that could have appeared to influence the work reported in this paper.

Data availability

Data will be made available on request.

Acknowledgment

This work was supported by the National Natural Science Foundation of China (Grant Nos. 51776079 & 52076088).

References

[1] T.T. Hoang, J. Ku, Multiple-evaporator loop heat pipe, in: 53rd AIAA Aerospace Sciences Meeting, 2015, p. 0709.
[2] Y.F. Maydanik, Loop heat pipes, Appl. Therm. Eng. 25 (2005) 635–657.
[3] N. Putra, B. Ariantara, R.A. Pamungkas, Experimental investigation on performance of lithium-ion battery thermal management system using flat plate loop heat pipe for electric vehicle application, Appl. Therm. Eng. 99 (2016) 784–789.
[4] H. Zhang, G. Li, L. Chen, G. Man, J. Miao, X. Ren, J. He, Y. Huo, Development of Flat-Plate Loop Heat Pipes for Spacecraft Thermal Control, Microgravity Sci. Technol. 31 (2019) 435–443.
[5] Y.F. Maydanik, M.A. Chernysheva, V.G. Pastukhov, Review: Loop heat pipes with flat evaporators, Appl. Therm. Eng. 67 (2014) 294–307.
[6] Z. Liu, D. Wang, C. Jiang, J. Yang, W. Liu, Experimental study on loop heat pipe with two-wick flat evaporator, Int. J. Therm. Sci. 94 (2015) 9–17.
[7] J. Li, D. Wang, G.P. Peterson, Experimental studies on a high performance compact loop heat pipe with a square flat evaporator, Appl. Therm. Eng. 30 (2010) 741–752.
[8] H. Song, L. Zhi-chun, Z. Jing, J. Chi, Y. Jin-guo, L. Wei, Experimental study of an ammonia loop heat pipe with a flat plate evaporator, Int. J. Heat Mass Transf. 102 (2016) 1050–1055.
[9] K. Odagiri, H. Nagano, Heat transfer characteristics of flat evaporator loop heat pipe under high heat flux condition with different orientations, Appl. Therm. Eng. 153 (2019) 828–836.
[10] Z. Zhang, H. Zhang, Z. Ma, Z. Liu, W. Liu, Experimental study of heat transfer capacity for loop heat pipe with flat disk evaporator, Appl. Therm. Eng. 173 (2020), 115183.
[11] R. Zhao, Z. Zhang, S. Zhao, H. Cui, Z. Liu, W. Liu, Experimental study of flat-disk loop heat pipe with R1233zd(E) for cooling terrestrial electronics, Appl. Therm. Eng. 197 (2021), 117385.
[12] J. Li, G. Zhou, T. Tian, X. Li, A new cooling strategy for edge computing servers using compact looped heat pipe, Applied Thermal Engineering, 187 (2021) 116599 %@ 111359-114311.
[13] L. Fourgeaud, R. Mari, V. Dupont, C. Figus, Experimental investigations of a Multi-Source Loop Heat Pipe for electronics cooling, Joint 19th IHPC and 13th IHPS, Pisa, Italy, 2018.
[14] Y.F. Maydanik, V.G. Pastukhov, M.A. Chernyshova, A.A. Delil, Development and Test Results of a Multi-Evaporator-Condenser Loop Heat Pipe, in: AIP Conference Proceedings, Vol. 654, American Institute of Physics, 2003, pp. 42-48.
[15] Y. Qu, S. Wang, Y. Tian, A review of thermal performance in multiple evaporators loop heat pipe, Appl. Therm. Eng. 143 (2018) 209–224.
[16] Y. Maidanik, Y. Fershtater, V. Pastukhov, K. Goncharov, O. Zagar, Y. Golovanov, Thermoregulation of loops with capillary pumping for space use, SAE Trans. (1992) 523–528.
[17] W. Bienert, D. Wolf, M. Nikitkin, Y.F. Maidanik, Y. Fershtater, S. Vershinin, J.M. Gottschlich, Proof-of-feasibility of multiple evaporator loop heat pipes, in: Sixth European Symposium on Space Environmental Control Systems, vol. 400, 1997, pp. 393.
[18] D. Bugby, K. Wrenn, D. Wolf, E. Kroliczek, J. Yun, S. Krein, D. Mark, Multi-evaporator hybrid loop heat pipe for small spacecraft thermal management, in: 2005 IEEE Aerospace Conference, IEEE, 2005, pp. 810-823.
[19] D. Bugby, Multi-Evaporator Hybrid Two-Phase Loop Cooling System for Small Satellites, 2007.
[20] J. Yun, D. Wolf, E. Kroliczek, T. Hoang, Multiple evaporator loop heat pipe, SAE Technical Paper (2000).
[21] S. Okutani, H. Nagano, S. Okazaki, H. Ogawa, H. Nagai, Operating Characteristics of Multiple Evaporators and Multiple Condensers Loop Heat Pipe with Polytetrafluoroethylene Wicks, JECTC 04 (01) (2014) 22–32.
[22] Y. Qu, D. Zhou, S. Qiao, K. Zhou, Y. Tian, Experimental study on the startup performance of dual-evaporator loop heat pipes, Int. J. Therm. Sci. 170 (2021), 107168.
[23] Y. Qu, S. Qiao, D. Zhou, Steady-state modelling of dual-evaporator loop heat pipe, Appl. Therm. Eng. 193 (2021), 116933.
[24] X. Chang, N. Watanabe, H. Nagano, Visualization study of a loop heat pipe with two evaporators and one condenser under gravity-assisted condition, Int. J. Heat Mass Transf. 135 (2019) 378–391.
[25] N. Phan, Y. Saito, N. Katayama, H. Nagano, Operating characteristics of a dual flat-evaporator loop heat pipe for single heat source cooling in any orientation, Int. J. Heat Mass Transf. 172 (2021), 121146.
[26] M. Kaviany, Principles of heat transfer in porous media, Springer Science & Business Media, 2012.
[27] Y. Qu, S. Qiao, D. Zhou, Steady-state modelling of dual-evaporator loop heat pipe, Appl. Therm. Eng. 193 (2021) 116933 %@ 111359-114311.

[28] J. Ku, G.C. Birur, An experimental study of the operating temperature in a loop heat pipe with two evaporators and two condensers, SAE Technical Paper (2001).
[29] Y.F. Maydanik, S.V. Vershinin, M.A. Chernysheva, Experimental study of an ammonia loop heat pipe with a flat disk-shaped evaporator using a bimetal wall, Appl. Therm. Eng., 126 (2017) 643-652 %@ 1359-4311.
[30] Z. Zhang, H. Zhang, X. Lai, Z. Liu, W. Liu, Numerical study on thermohydraulic behavior in compensation chamber of a loop heat pipe with flat evaporator, Appl. Therm. Eng. 171 (2020), 115073.